

High-Throughput, Energy-Efficient RRAM-Based In-Memory Computing LPN Accelerator

Hao Yue

University of Chinese Academy
of Sciences
Beijing, China
yuehao22@mails.ucas.ac.cn

Zhelong Jiang

University of Chinese Academy
of Sciences
Beijing, China
jzl@semi.ac.cn

Zhigang Li

Institute of Semiconductors,
Chinese Academy of Sciences
Beijing, China
lizhg@semi.ac.cn

Yihao Chen

University of Chinese Academy
of Sciences
Beijing, China
chenyihao97@semi.ac.cn

Gang Chen*

Institute of Semiconductors,
Chinese Academy of Sciences
Beijing, China
chengang08@semi.ac.cn

Huaxiang Lu

Institute of Semiconductors,
Chinese Academy of Sciences
Beijing, China
luhx@semi.ac.cn

Abstract—As a strong candidate for the post-quantum cryptographic (PQC) era, Learning Parity with Noise (LPN) has been extensively studied in the field of cryptography. However, the data transfer bottleneck between the computation and memory modules has significantly hindered the development of LPN-based cryptographic techniques due to large matrices. This work introduces an RRAM-based in-memory computing LPN accelerator aimed at overcoming data transfer bottlenecks, thereby executing LPN computation tasks efficiently. To ensure the high accuracy of the LPN AND operation, a folded current amplification circuit is proposed to address the leakage current issue caused by the limited high-resistance state of RRAM. Meanwhile, a Cumulative XOR Fast Computing Method is introduced to efficiently convert accumulated current values into LPN XOR operation results.

Index Terms—Learning Parity with Noise (LPN), In memory, computing, RRAM, Transmission bottleneck

I. INTRODUCTION

In recent years, post-quantum encryption (PQC) has grown rapidly for its potential to resist brute-forcing decryption threats enabled by progressively feasible quantum computers. Among the numerous candidates for PQC, Learning Parity with Noise (LPN) stands out due to its concise arithmetic structure and provable security against both classical attacks and quantum attacks [1]. However, despite the LPN's great theoretical success in studying cryptographic primitives and protocols, it has not been as widely implemented in actual cryptographic systems as other lattice-based post-quantum cryptosystems like Crystals-Kyber [2]. A primary reason for this issue is that the LPN task involves the transmission of a large public matrix. When executing the LPN task, the conventional Von Neumann computing architectures require the transfer of large public matrices between distinct computing and memory units. This process not only consumes substantial energy but also introduces considerable computational latency. This is unacceptable for applications that require real-time performance and low power consumption. Therefore, the primary challenge in designing an efficient LPN accelerator is how to

overcome the bottleneck of transferring large public matrices between the computation and memory modules.

LPN exhibits simple data characteristics and arithmetic operations, with its data distributed in the binary field, requiring only AND and XOR operations to perform all computations. However, the data volume is large, representing a large-scale public matrix computation. It is essential to fully leverage these characteristics of LPN when designing and selecting the hardware architecture for an efficient LPN accelerator. In-memory computing (IMC) [3], a promising architecture designed to overcome the Von Neumann bottleneck, shows significant potential for efficiently solving the LPN problem. The in-memory computing architecture not only has a natural advantage in executing simple arithmetic operations, but also significantly improves data transfer efficiency, breaking the bottleneck between computation and memory modules, thereby greatly enhancing the computational efficiency of LPN. It is believed that the IMC architecture aligns well with the computational characteristics of LPN. Therefore, the IMC architecture is an ideal choice for executing LPN operations.

Inspired by the above motivation, in this study, an LPN accelerator based on processing-in-memory architecture using Resistive Random-Access Memory (RRAM) is proposed. The RRAM-based in memory computing LPN accelerator directly performs all LPN operations, namely AND and XOR, within the memristor array. Consequently, this architecture eliminates the need for data transfer between the computation and memory modules, thereby overcoming the data transfer bottleneck and fundamentally enhancing the computational efficiency of LPN. Meanwhile, to improve the computation accuracy and efficiency of LPN within the memristor array, this study has made efforts in two areas: 1) high-precision implementation of AND operations. To address the accuracy issues caused by the limited high resistance of memristors, a folded current amplification circuit to increase the equivalent impedance of the high-resistance state of the memristor was

designed, thereby improving the accuracy of the output current obtained after the AND operation; 2) efficient implementation of XOR operations. A Cumulative XOR (CXOR) Fast Computing Method (CFCM) is proposed to efficiently convert accumulated current values into LPN XOR operation results.

The remaining part of this paper is organized as follows. Section II introduces the background knowledge of LPN and RRAM, followed by the circuit mapping relationship between LPN and RRAM in this work. Section III provides a detailed introduction of the hardware architecture of the LPN accelerator, including the architecture implementation, data flow, and the realization of key modules. Then, Section IV presents the measured results. Finally, the work presented in this paper is summarized in Section V.

II. BACKGROUND KNOWLEDGE AND CIRCUIT MAPPING

A. Characteristics of RRAM

The defining characteristic of RRAM is that the resistance of the memristor can be altered when a pulse voltage is applied across its terminals. Thus, by controlling the pulse voltage applied across the device, the memristor's resistance state can be manipulated to be either a high-conductance state (HCS) or a low-conductance state (LCS). Additionally, RRAM is a non-volatile device that maintains its resistance value for a long period after it has been set, even in the absence of power. Moreover, memristors support repeated resistance write operations. Due to these characteristics, RRAM has been widely adopted in processing-in-memory applications [3].

B. The Computing Paradigm of the LPN

Recently, the applications of LPN in cryptography have been widely researched. Many LPN-based cryptographic schemes have been gradually developed. Here, taking the standard LPN cryptographic scheme as an example, the basic computational paradigm of LPN is introduced. Due to space limitations, more details are provided in [4].

Standard LPN Encryption [5]: Let \mathbb{F}_2^k represent k -dimensional space, where the data is distributed only in the binary field. \oplus represents the XOR operation between two binary elements, and \cdot represents the AND operation between two binary elements. In the computational paradigm of LPN, the AND operation has a higher precedence than the XOR operation. The standard LPN encryption scheme consists of three following algorithms:

- KeyGen ($\mathbf{1}^{sec}$): Given a security parameter sec , sample a secret key $\mathbf{s} \in \mathbb{F}_2^n$ uniformly at random.
- Enc (\mathbf{m}, \mathbf{s}): Given a message $\mathbf{m} \in \mathbb{F}_2^m$ and the secret key \mathbf{s} , uniformly sample a random matrix $\mathbf{A} \in \mathbb{F}_2^{m \times n}$ and an error vector $\mathbf{e} \in \mathbb{F}_2^m$, $\mathbf{G} \in \mathbb{F}_2^{m \times c}$ represents a generator matrix. We obtain the ciphertext output $\mathbf{b} = \mathbf{A} \cdot \mathbf{s} \oplus \mathbf{e} \oplus \mathbf{G} \cdot \mathbf{m}$.
- Dec ($(\mathbf{A}, \mathbf{b}), \mathbf{s}$): Given a ciphertext (\mathbf{A}, \mathbf{b}) and the secret key \mathbf{s} , compute $\mathbf{b} \oplus \mathbf{A} \cdot \mathbf{s}$ and apply a decoding algorithm to recover \mathbf{m} .

From the LPN formulas above, it is evident that both the encryption and decryption processes fundamentally involve

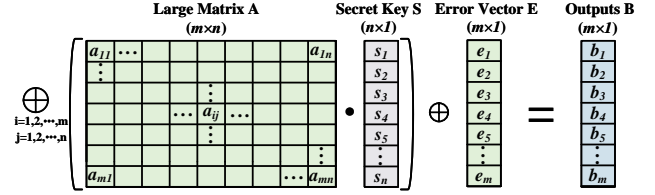


Fig. 1. Enter Caption

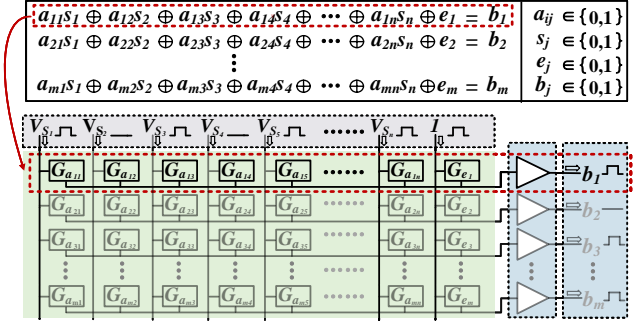


Fig. 2. The mapping relationship between LPN and circuit

XOR and AND operations between elements of matrices and vectors. Therefore, it can be demonstrated that the basic computational paradigm of LPN can be summarized as:

$$b_i = \left(\bigoplus_{j=1,2,\dots,n} a_{ij} \cdot s_j \right) \oplus e_i, i \in \{1, 2, \dots, m\}, (1)$$

where \oplus denotes the XOR operation and \cdot denotes the AND operation, as illustrated in Fig.1.

C. Circuit Mapping of LPN

Fig.2 illustrates the circuit mapping of LPN operations onto the processing-in-memory accelerator based on RRAM. The LPN operation can be expressed as $\mathbf{b} = \mathbf{A} \cdot \mathbf{s} \oplus \mathbf{e}$. For the i -th row, the operation that needs to be performed is shown in equation (1). When mapping logic from LPN to RRAM arrays, the input pulse vector of the array represents \mathbf{s} , and the output pulse vector corresponds to the result vector \mathbf{b} . A high pulse represents logic 1, while the absence of a pulse represents logic 0. The elements of the large matrix \mathbf{A} and the error vector \mathbf{e} are encoded as the conductance values of RRAMs. For instance, if the matrix element a_{ij} is 1, the RRAM $G_{a_{ij}}$ corresponds to the high conductance state; if the a_{ij} is 0, $G_{a_{ij}}$ is programmed to the low conductance state.

III. PROPOSED IN MEMORY COMPUTING ARCHITECTURE

A. Data Flow of LPN in the RRAM Accelerator

Fig.3 illustrates the data flow of LPN computation implementation in RRAM accelerator. The LPN operation is primarily divided into two steps: 1) an AND operation between two elements is performed to obtain the output current, and 2) the output current is then accumulated for a XOR operation to obtain the final output result. The two-element AND operation

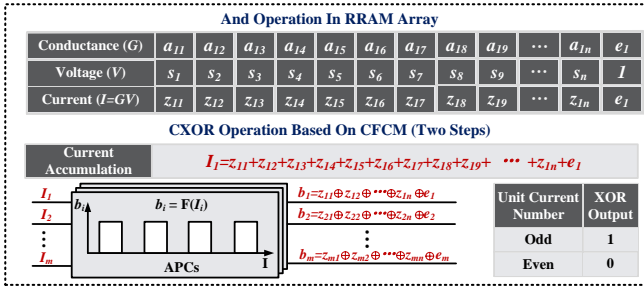


Fig. 3. Data flow of LPN in the RRAM Accelerator

LPN is implemented based on Ohm's law. Taking s_j and a_{ij} as examples, when $a_{ij} \cdot s_j$ equals 1, the magnitude of current z_{ij} equals the unit current $4\mu\text{A}$; when $a_{ij} \cdot s_j$ equals 0, the magnitude of current z_{ij} is $0\mu\text{A}$. Regarding Cumulative XOR (CXOR) operations, a CXOR Fast Computing Method (CFCM) more suitable for RRAM arrays was proposed. CFCM is designed based on an intuitive observation that the CXOR value depends on the parity of the Hamming weight of result vector \mathbf{b} . For instance, when the Hamming weight is odd, the CXOR value is 1, and when that is even, the CXOR value is 0. In terms of computing circuits, CXOR computation based on CFCM is implemented in two steps. The first step involves accumulating the AND current to obtain the summed current I_{sum} , which represents the Hamming weight of the output current vector. The second step involves utilizing several Analog Parity Checkers (APCs) to convert I_{sum} into the corresponding CXOR value. Specifically, when I_i is an odd number of units, CXOR is 1; when I_i is an even number of units, CXOR is 0. CFCM fully utilizes the RRAM computation array's power in performing accumulation operations. This can assist the computation macro in reducing the power consumption and computation delay associated with the extensive use of sense amplifiers (SA) and XOR logic gates.

B. Architecture of the Accelerator

In this section, a detailed description of the proposed processing-in-memory architecture is provided. As shown in Fig.4, the architecture of the proposed LPN accelerator primarily consists of a Secret Key Input Driver, an Address Controller, a Mode Controller, an XOR Logic Circuit, an Output Buffer, and four RRAM arrays. The Address Controller and Mode Controller are used to control the RRAM write driver and RRAM read buffer in the RRAM arrays to facilitate weight writing and reading. The Secret Key Input Driver, Output Buffer, XOR Logic Circuit, and RRAM arrays are the primary circuit units for LPN computations. As depicted in the Fig.4, both AND and XOR operations of the LPN computation paradigm are performed directly within the memristor array. In an RRAM array, each memristor unit performs the AND operation with the inputs, producing an output current. This current is summed across the entire row and then enters the

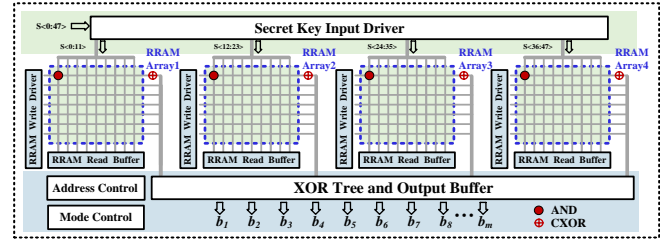


Fig. 4. Overall architecture of LPN acceleration

APC module to complete the conversion from the accumulated current value to the XOR operation result.

The illustrative parameters were used to simplify the description of the scale of the RRAM array. Assume that one RRAM array can deploy LPN computations of size 512×12 . Four RRAM arrays' computation results can be concatenated via an XOR Tree. Meanwhile, this RRAM-based processing-in-memory architecture is highly parallel. Thus, this accelerator can complete 512×48 LPN computations within a single clock cycle $1\mu\text{s}$. For larger-scale LPN computations, an accelerator tree architecture can support them.

C. High-Precision Implementation of MAC Operations

Since RRAM arrays inherently possess the capability to perform current accumulation, achieving high-precision multiply-accumulate operations essentially equates to achieving high-precision multiplication, specifically the AND operation in LPN. Therefore, the output current accuracy of each logical AND unit in the RRAM array after computation should be high enough to improve the computational precision of LPN.

Fig.5(a) illustrates the specific implementation circuit of the RRAM-based logic AND unit in the proposed accelerator. During the AND operation, the input signal V_{s_j} affects the gate of the PMOS in the 1T1R structure after passing through an inverter. Compared to the traditional 1T1R structure, the proposed RRAM computing unit incorporates a folded current amplify structure at the drain side of M1 within the 1T1R.

This structure serves two purposes. Firstly, it mitigates the leakage current issue caused by the limited resistance value of memristors in the high resistance state (HRS). As shown in Fig.5(b), the limited high-resistance value means that the conductance G_{LCS} of memristors in the low conductance state is not zero. When the input signal s_j activates transistor M1, the input is equivalent to logic 1, resulting in the unit outputting a leakage current that deviates from the ideal condition. This may cause overlapping ranges of accumulated currents corresponding to different MAC values, thereby impacting the conversion accuracy of the APC module and ultimately affecting the final XOR result. The folded current amplification structure can lower the gate-source voltage of the output transistor when the memristor is in the low-conductance state, thereby significantly reducing the output leakage current. Additionally, it addresses the instability of the on/off ratio due to read disturbances in the memristor.

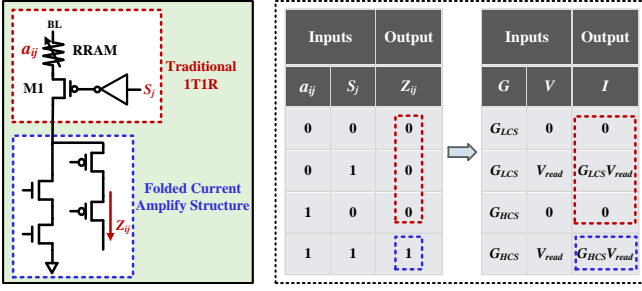


Fig. 5. (a) RRAM-based Logic AND unit (b) Data correspondence diagram

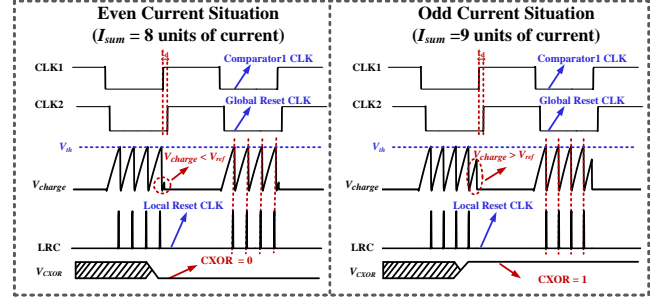


Fig. 7. The waveform diagram of APC

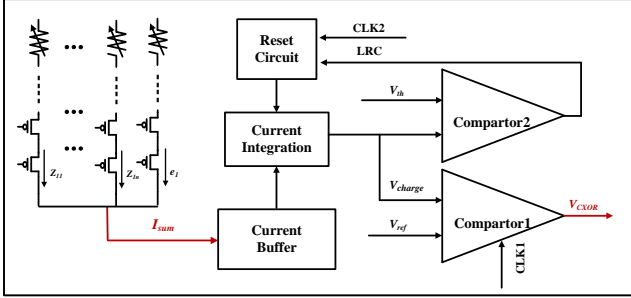


Fig. 6. Overall Structure of APC

D. Implementation of APC

Fig.6 displays the implementation scheme of the proposed analog parity checker. The APC primarily consists of a current buffer, two comparators, a reset circuit, and a current integration circuit. The current buffer not only ensures the complete transfer of I_{sum} to the current integration circuit but also shields its input, which experiences significant voltage fluctuations from the output of the RRAM array. This isolation stabilizes the output current of the RRAM array and enhances conversion accuracy. Fig.7 presents the waveform of the APC module. When CLK2 is low, the current integration circuit charges the internal capacitor based on the magnitude of I_{sum} , and outputs a ramp waveform under the influence of Comparator2 and the Reset Circuit. Within the conversion cycle, the number of ramp waves is equal to the half number of unit currents in I_{sum} . The operating clock of the comparator1, CLK1, is meticulously designed to slightly precede the global reset clock, CLK2, by a small duration t_d . During this time t_d , if V_{charge} exceeds V_{ref} , then I_{sum} is an odd number of unit currents, resulting in an output of 1 from V_{CXOR} ; otherwise, V_{CXOR} outputs 0.

IV. RESULTS

Fig.8 shows the test results related to the precision of the multiply-accumulate (MAC) operation. Two main factors affect the precision: 1) fluctuations in the conductance value (G_{HCS}) of the RRAM in the high-conductance state, which cause variations in the output current when the input is equivalent to logic 1; 2) leakage current resulted from the

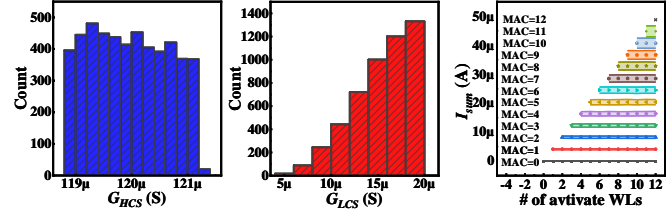


Fig. 8. Test results related to the precision of MAC operation

non-zero conductance value (G_{LCS}) of the RRAM in the low-conductance state. As previously discussed, the folded current amplification circuit effectively suppresses the impact of leakage current. From Fig.10 (left and center), it can be observed that in practical deployment, the G_{HCS} of the RRAM is precisely programmed to 120 μS , maintaining conductance fluctuations at the level of 1%, while the G_{LCS} of the RRAM is programmed to be less than 20 μS . Benefiting from the above results and the use of the folded current amplifier circuit, as shown in the right side of Fig.8, although the fluctuations in I_{sum} are positively correlated with the number of units involved in the multiply-accumulate operation, there is no significant overlap in I_{sum} corresponding to different MAC values. Therefore, a subarray can achieve high-precision accumulation of output currents from no more than 12 logic AND units.

Fig.9 illustrates the programming bit error rate of the memristor resistance and the computation bit error rate of the LPN accelerator in actual deployment. During the actual 98,304 programming cycles, the RRAM encountered errors in a total of 37 cycles, achieving a correct programming rate of 3.76E-4. In the actual 2048 output bits, the macro-level LPN computation accuracy was 99.3%, thanks to the inherent fault tolerance of LPN operations.

V. CONCLUSION

This work proposes an LPN accelerator based on a processing-in-memory architecture, aiming to break the data transfer bottleneck between the computation and memory modules caused by large public matrices. Based on the data characteristics and computational paradigm of LPN, a high-

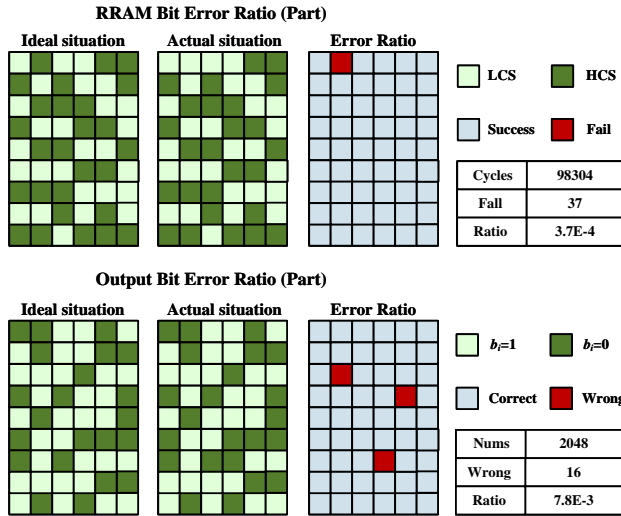


Fig. 9. The bit error rate of weight programming and LPN computation

precision MAC operation scheme and a CXOR fast computing method better suited for RRAM arrays are proposed, thereby enhancing both the computational accuracy and efficiency of the LPN accelerator.

ACKNOWLEDGMENT

This work was supported in part by the CAS Strategic Leading Science and Technology Project XDB44000000 and in part by the National Natural Science Foundation of China 92364202.

REFERENCES

- [1] Blum A., Kalai A., Wasserman H., "Noise-tolerant learning, the parity problem, and the statistical query model", *Journal of the ACM (JACM)*, 2003:506-519.
- [2] Ben-Efraim A., Cong K., Omri E., et al., "Large scale, actively secure computation from LPN and free-XOR garbled circuits", *Annual International Conference on the Theory and Applications of Cryptographic Techniques*. Cham: Springer International Publishing, 2021:33-63.
- [3] Imani M., Gupta S., Kim Y., et al., "Floatpim: In-memory acceleration of deep neural network training with high precision", *Proceedings of the 46th International Symposium on Computer Architecture*. 2019:802-815.
- [4] A. Ben-Efraim et al., "Large Scale, Actively Secure Computation from LPN and Free-XOR Garbled Circuits," in *EUROCRYPT*, 2021.
- [5] Nejatollahi H., Gupta S., Imani M., et al., "Cryptopim: In-memory acceleration for lattice-based cryptographic hardware", *2020 57th ACM/IEEE Design Automation Conference (DAC)*. IEEE, 2020:1-6.
- [6] Ding L., Bian S., Zhang J., "PIMA-LPN: Processing-in-memory Acceleration for Efficient LPN-based Post-Quantum Cryptography", *2023 60th ACM/IEEE Design Automation Conference (DAC)*. IEEE, 2023:1-6.